A Wideband Digital Predistortion Based on Adaptive Subband Decomposition Technique

Xiaofang Wu，Miao Xiong

***Abstract*—**In wideband communication systems, conventional predistortion techniques suffer from correction bandwidth limitation, which implies that the linearization performance will deteriorate when the signal bandwidth expands. In this paper, a subband predistortion structure is proposed, aiming at correcting the dynamic nonlinear distortion of wideband power amplifiers. The predistortion is composed of an adaptive memoryless lookup table followed by an adaptive subband linear filterbank. The former is used to compensate for the nonlinearity of power amplifiers, and the latter is used to compensate for the memory effects of power amplifiers. In addition, the identification algorithm of the subband predistortion is described, taking account of coordinating the two adaptive modules. Simulation results show that the proposed predistortion can remarkably suppress the nonlinear distortion with about 20dB's ACPR reduction. The comparative results of a four-subband-filter case and a full-band-filter case show that the subband predistortion has better linearization performance, as well as faster convergence speed due to the smaller correlation of each subband signals.

***Keywords*—**digital predistortion, adaptive filtering, subband decomposition, identification, power amplifier

I. Introduction

In recent years, new standards enhancing high data rates by means of spectrally-efficient complex modulation schemes are tending to be applied in modern communication systems, which results in power amplifiers (PAs) in the RF transmitter chains handling signals that present high peak-to-average power ratios (PAPRs). However, these high PAPR modulation formats are very sensitive to the intermodulation distortion of the PAs. In order to satisfy the mandatory linearity requirements in communication standards, significant backoff (BO) levels of operation are required, thus penalizing power efficiency in the PAs. Therefore, there exists contradiction between high efficiency and good linearity. A popular solution to avoid the power inefficient BO operation (increase power efficiency while keeping good linearity) is the use of PA linearizers.

Besides the efficiency problem, when the signal bandwidth increases, memory effects will appear due to the PA's intrinsic dynamics, which implies that the amplified signal not only depends on the input signal at the same time instant, but also on the history of the input signals as well. In the literature [1]-[3], two categories of memory effects have been identified, which are electrical and electro-thermal memory effects. The main factor that causes electrical memory effects is the variation of terminal impedances (biasing and matching circuit's impedances) over the input signal bandwidth around the carrier frequency and its harmonics, as well as at the baseband frequency. On the other hand, temperature effects, traps and aging lead to electrothermal memory effects. With the bandwidth increases, the memory effects will increase too, and the performance of PA linearizers will degrade. Therefore memory effects have to be moved away by the linearizers especially in wideband applications.

Among linearizers, digital predistortion (DPD) is becoming one of the mainstream linearization techniques due to the rapid development of digital signal processing (DSP) techniques [4]-[8]. Different predistortion techniques, which are intended to compensate for the nonlinearity as well as the memory effects, have been reported in the literature. For example, box-oriented models, such as Hammerstein or Wiener, are widely used for their explicit structures to describe the cascaded nonlinearity and memory effects [9]-[11]. Besides, the lookup table (LUT) based method has been another important branch of DPD techniques for its low cost of hardware realization [12][13]. Although these conventional techniques are powerful, they suffer from a correction bandwidth limitation problem due to the required computation complexity, which implies that the linearization performance will deteriorate when the signal bandwidth expands [14]. In [14], a subband predistorter was proposed to solve this problem by dividing the wideband signal into several narrow-band signals. The predistorter can be seen as a hybrid structure of LUT and Hammerstein. Concretely, it consists of a cascade of a static LUT-based predistorter followed by an adaptive subband filterbank. The subband technique brings two major benefits, the reduction of the length of linear subband filters and the improvement of the adaptive convergence speed. However, due to the use of a static LUT, this structure can only compensate for temperature drift in a long period, i.e. electrothermal memory effect. But as mentioned above, in wideband communication systems, electrical memory effect plays a predominant role and breeds short-time dynamic drift of nonlinear characteristic of PA. Therefore, in this paper, we will

This work was supported in part by the Natural Science Foundation of China under Grant 61201195.

Xiaofang Wu is with the School of Information Science and Technology, Xiamen University, Xiamen, China (corresponding author to provide e-mail: xfwu@ xmu.edu.cn).

Miao Xiong is with the School of Information Science and Technology, Xiamen University, Xiamen, China (e-mail: 690965960@qq.com).

introduce an improved subband based predistortion, devoting to correcting the dynamic nonlinear behavior of power amplifiers.

The paper is organized as follows. In Section Ⅱ, the subband filtering technology is briefly presented. The proposed subband predistorter and its adaptive algorithm are described in Section Ⅲ. The Matlab simulation results of the proposed predistortion are demonstrated in Section Ⅳ. Finally, conclusions are drawn in Section Ⅴ.

II. Subband Filtering Technology

A structure of *L*-channel filter bank is shown in Fig. 1, it is composed of two stages, which are the analysis stage and the synthesis stage. In Fig. 1, $x(k)$ is the input signal and $\hat{x}(k)$ is the output signal, while $\{h_l(k), l=0,1,\ldots,L-1\}$ is the analysis filter bank and $\{f_l(k), l=0,1,\ldots,L-1\}$ is the synthesis filter bank. $\downarrow D$ and $\uparrow D$ respectively represent decimator and interpolator where D ($D \le L$) is the factor of decimator (interpolator). $D = L$ refers to the critically sampling case, and $D < L$ refers to the oversampling case. Since critically sampled filter banks have contradiction between stop-band attenuation and aliasing inhibition, whereas over-sampled filter banks which introduce redundancy can solve this problem very well, so we use over-sampling in the following simulations. In Fig. 1, the analysis filter bank divides the input signal $x(k)$ into L subband signals uniformly, and then the signals are extracted with the ratio D. On the other side, the subband signals are interpolated by the same ratio D to recover sampling rate and the synthesis filter bank is used to remove mirror components produced by interpolating. Finally, by adding all of the subband signals we can get the full-band output $\hat{x}(k)$. When $\hat{x}(k)$ is equivalent to the input signal $x(k)$ with a pure time delay, i.e., $\hat{x}(k) = cx(k-d)$, where c and d are constants, we call $\hat{x}(k)$ is the perfect reconstruction (PR) of $x(k)$.

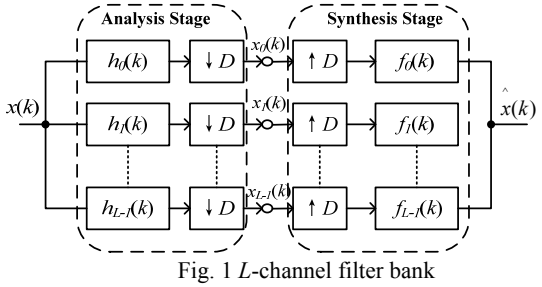

Fig. 1 *L*-channel filter bank

In the system shown in Fig. 1, the main distortion of $\hat{x}(k)$ versus $x(k)$ usually divides into three kinds: aliasing distortion, amplitude distortion and phase distortion. Therefore, in order to ensure the perfect reconstruction of the filter bank, the key to design filter bank is to eliminate these distortions. We uses the cosine-modulated filter bank (CMFB) which is modulated by a low-pass prototype filter, thus the optimization problem of the filter bank can be simplified to a low-pass prototype filter's optimization problem. We suppose the *L*-channel cosine-modulated filter bank is built on a low-pass prototype filter function $h(n)$ with the cut-off frequencies $\pm\pi/2L$ and the length N. So the functions of analysis filter bank and synthesizing filter bank are as follows:

$$h_k(n) = 2h(n)\cos[(k+0.5)(n-\frac{N-1}{2})\frac{\pi}{L} + (-1)^k \pi/4] \quad (1)$$

$$g_k(n) = 2h(n)\cos[(k+0.5)(n-\frac{N-1}{2})\frac{\pi}{L} - (-1)^k \pi/4] \quad (2)$$

i.e., $h_k(n)$ and $g_k(n)$ are modulated by $h(n)$ with shift $\frac{\pi}{2L} + k\frac{\pi}{L}$, where $k = 0,1,2,\cdots,L-1$. The filter bank got from (1) and (2) can achieve linear phase, so we only need to eliminate amplitude distortion and aliasing distortion. We use linear iterative optimization method [15] to design the prototype low-pass filter, whose advantage is transforming the nonlinear optimization problem into an optimization problem of linear equation, thus the computational complexity can be reduced.

III. Subband Digital Predistortion

The proposed structure of the subband digital predistortion is shown in Fig. 2. The predistorter consists of a memoryless adaptive lookup table (LUT) module and a subband adaptive filter bank module. The latter is formed by interposing a processing stage to the *L*-channel filter bank described in Section Ⅱ, i.e., it is a cascade of the analysis stage, the processing stage and the synthesis stage. The LUT is used to compensate for the nonlinearity of power amplifier, and the subband adaptive filter bank is designed to compensate for the memory effects of power amplifier, where $F_l(z), l=0,1,\ldots,L-1$ is the linear finite impulse response (FIR) filter. The DPD-PA system has $u(n)$ as its input and $z(n)$ as its output. When the adaptive algorithm converges, ideally, we will get $z(n) = Gu(n-\tau) = Gd(n)$, where G is the gain of the linearized PA, and τ is the delay of the forward predistorter-PA path.

Compared with the subband predistortion structure in [14], the proposed structure has two advantages: First, since the LUT in [14] always keeps stationary and only the subband processing stage adaptively updates to mitigate the slow temperature drift of a PA, the subband predistortion in [14] can only be used to compensate for electro-thermal memory effects of the PA. However, in the context of a wideband wireless PA, the electric memory effects are the dominant sources of the memory effects since the thermal filter time constant is too large compared to the inverse of the signal bandwidth [3]. In this paper, the LUT is adaptive, so the predistorter can effectively compensate for the PA's dynamic nonlinear variation, especially the electrical memory effects. Second, in [14], the analysis and synthesis filter banks have a tree structure cascaded by two-channel orthogonal mirror filter bank (QMFB). Since the aliasing components carried by each subband signals have to be eliminated by suitable filters, it is a tough job to

design the QMFB filters. On the contrary, the advantage of using nearly reconstructed CMFB in our paper is that by modulating a prototype low-pass filter to get the filter coefficients in L channels, it can reduce the difficulty of filter bank design.

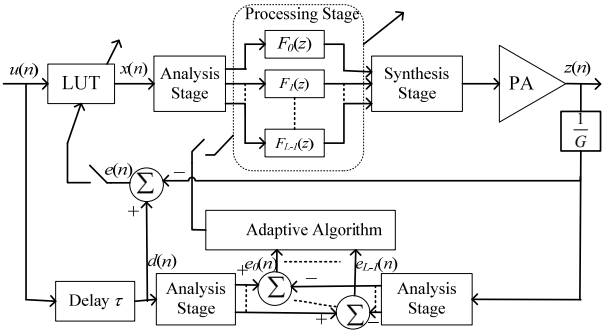

Fig. 2 Structure of the subband digital predistortion

A. Adaptive Polar Lookup Table Module

In this paper, the LUT method uses polar lookup table algorithm and contains two one-dimensional predistortion tables. The tables store amplitude compensation information and phase compensation information as shown in Fig. 3. First the input signal $u(n)$ goes through a rectangle/polar (r/p) transformation to get its amplitude $\rho(n)$ and phase $\varphi(n)$, and adds to the predistorter. Then the LUT index address is obtained from uniform quantization of the input power:

$$\begin{aligned} X &= Int\left(\frac{\rho^2(n)}{P_{\max}}\cdot L_x\right) && \rho(n) < \sqrt{P_{\max}} \\ X &= L_x - 1 && \rho(n) \ge \sqrt{P_{\max}} \end{aligned} \tag{3}$$

where $\rho^2(n)$ is the power of input signal, $P_{\max}$ represents the ideal power upper value and L_x is the size of the lookup table. Thus, the address X is an integer among $0,1,\cdots,L_x-1$. By addressing, the LUT predistorter obtains amplitude and phase compensation signals. At last the corrected amplitude signal $r(n)$ and phase signal $\theta(n)$ are transformed by polar/rectangle (p/r) and we get the LUT predistorter's output signal $x(n)$. In Fig. 3, $z(n)$ is the output signal of the PA, whose amplitude and phase are $R(n)$ and $\psi(n)$ respectively. The LUT linearization goal is:

$$\begin{aligned} R(n) &= \begin{cases} G\rho(n) & \rho(n) \le \sqrt{P_{\max}} \\ A_{sat} & \rho(n) > \sqrt{P_{\max}} \end{cases} \\ \psi(n) &= \varphi(n) \end{aligned} \tag{4}$$

where G is the expected linear gain, and $P_{\max}$ is the upper limit of the input power.

The LMS adaptive algorithm [16] is used to update LUT:

$$\begin{aligned} H_R(\rho(n))_{n+1} &= \begin{cases} H_R(\rho(n))_n - \alpha(R(n) - G\rho(n)) & \rho(n) \le \sqrt{P_{\max}} \\ A_{sat} / \rho(n) & \rho(n) > \sqrt{P_{\max}} \end{cases} \\ H_\theta(\rho(n))_{n+1} &= H_\theta(\rho(n))_n - \beta(\psi(n) - \varphi(n)) \end{aligned} \tag{5}$$

where $H_R(\bullet)$ and $H_\theta(\bullet)$ represent the amplitude signal and the phase signal of LUT respectively, and α and β are the step sizes of iterations.

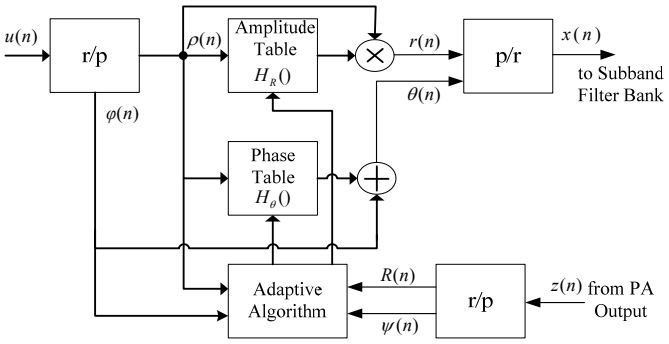

Fig. 3 Structure of the polar lookup table

B. Subband Adaptive Linear Filter Bank Module

The subband adaptive filter bank uses open-loop adaptive structure. As shown in Fig. 2, in the forward path, the output of LUT, $x(n)$, is decomposed into L subband signals $x_0(n),\cdots,x_{L-1}(n)$ by an analysis stage as (1), then the subband signals go through a linear filter bank $F_l(z), l = 0,1,\ldots,L-1$, which has the format of FIR as:

$$F_l(z) = \sum_{k=0}^{L_l-1} w_k z^{-k} \tag{6}$$

where L_l is the length of the lth subband filter, and w_k is the kth tap's weight needed to be estimate. The output of the FIR filters are synthesized by a synthesizing filter bank as (2), and then the whole-band signal is sent to the PA.

Also shown as in Fig. 2, in the feedback path, the delay signal $d(n) = x(n-\tau)$ is decomposed into L subband signals $d_0(n),\cdots,d_{L-1}(n)$ after going through the same analysis stage as in the forward path. The feedback signal $z(n)/G$ is also decomposed into L subband feedback signals $z_0(n),\cdots,z_{L-1}(n)$ after going through the same analysis stage. The error of each subband channel is $e_l(n) = d_l(n) - z_l(n)$. The subband LMS adaptive algorithm is as follows:

$$\mathbf{W}_l(i+1) = \mathbf{W}_l(i) + \mu_l \cdot \mathbf{X}_l(i) \cdot e_l^*(i) \tag{7}$$

where $\mathbf{W}_l(i) = [w_0^l,\cdots,w_{L_l-1}^l]^T$ is the weight vector of the lth subband FIR filter $F_l(z)$, $\mathbf{X}_l(i) = [x_l(i), x_l(i-1),\cdots, x_l(i-L_l+1)]$ and μ_l is the step size.

C. Adaptive Algorithm of the Subband Predistortion

Because the subband predistorter consists of two adaptive modules, it becomes an important issue to coordinate the two adaptive modules. Taking into account of the predistorter structure which can be regarded as an extended Hammerstein structure, we use Narendra-Gallman (NG) [9] iterative algorithm, a general learning algorithm for Hammerstein structure, as the adaptive algorithm of the whole predistorter. It has the advantage of low computational complexity. When

calculating the nonlinear module, the linear module is assumed to be still. Likewise, when calculating the linear module, the nonlinear module is assumed to be still. The LMS algorithms of the two modules work alternately until the two modules converge.

The steps of the NG adaptive algorithm are described below:

a. Initialize the amplitude table and the phase table of the LUT module. The amplitude values are set to be 1 and the phase values are set to be 0, which means that the LUT is an all-pass system. Initialize the weight vector of each subband FIR filters $W_l(0)$ to be $[1,0,\cdots 0]^T$, which means that the subband filter bank is an all-pass system too.

b. As shown in Fig. 2, there are two switches to control the on/off of the subband filter bank adaptive path and the LUT adaptive path respectively. Turn off the subband filter bank adaptive path to remain the filter bank still and turn on the LUT adaptive path simultaneously to update the LUT module by (5) until the table converges.

c. Alternately, turn off the LUT adaptive path and turn on the subband filter bank adaptive path at the same time, then updates the subband module by (7) until the filters converges.

d. Judge whether the system error $|e_{total}(n)|^2 = |z(n) - Gd(n)|^2$ reaches convergence threshold. If yes, stop the iteration; else, return to (2) and go on.

IV. Simulation Results

In the following simulations, the reconstruction performance of the CMFB filter bank is given, and the linearization performance of the proposed subband predistorter is assessed using a two-carrier WCDMA signal in Matlab environment. Furthermore, we compare and analyze the linearization and convergence performance of the subband predistorter and the conventional Hammerstein predistorter (which is also called full-band predistorter in this paper) .

A. Reconstruction Performance of the CMFB Filter Bank

The channel number of the CMFB filter bank (L) is set to be 4. We use the linear iterative optimization method [15] to design the low-pass prototype filter, and the tap number of the filter is set to be 64, and the energy ratio of pass-band and stop-band is set to be 10^4. Fig. 4 and Fig. 5 show the frequency response and amplitude distortion function of the CMFB analysis filter bank respectively. All of the results are measured after 25 iterations.

As we can see in Fig. 4 and Fig. 5, the design results show that the pass-band of analysis filter bank is very flat and it can reach -100dB stop-band attenuation, and the amplitude distortion is below 8×10^{-4}. Fig. 4 also illustrates that there are no overlaps between nonadjacent channels, that is to say, aliasing distortion doesn't exist. So we get the conclusion that the CMFB obtained by the linear iteration method is close to perfect reconstruction.

B. Linearization Performance of the Subband Predistortion

In the following simulations, we compare the linearization performance of the proposed subband predistortion model with the model in [14]. We choose the augmented Wiener PA model [17] for the sake that it describes the dynamic nonlinear behavior accurately. Fig. 6 is the block diagram of the augmented Wiener model, which is a cascade system with a dynamic memory module followed by a static nonlinear module. The dynamic memory module parallelizes two branches of FIR filters. The first branch is a FIR filter, which contributes the memory effects around the carrier frequency. The second branch multiplies the input signal's amplitude by the input signal and then the product goes through the second FIR filter, which contributes to the memory effects introduced by the non-ideal biasing and matching circuits. Therefore, the two-parallel-branch model represents the electronic memory effects accurately [17].

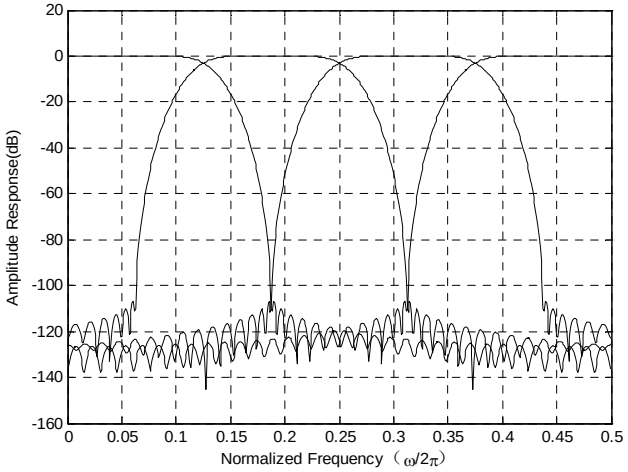

Fig. 4 Amplitude frequency response of the four-channel analysis filter bank

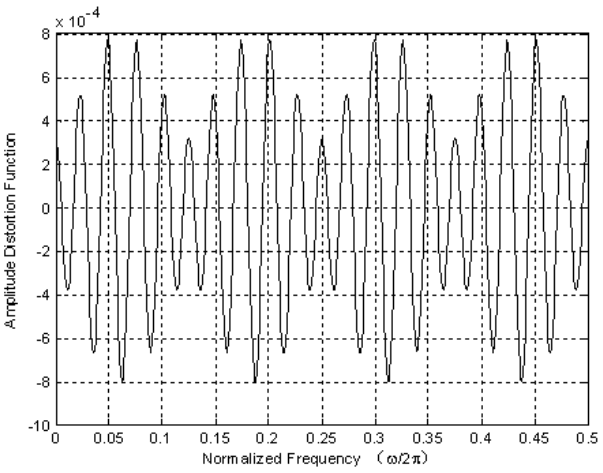

Fig. 5 Amplitude distortion function of the four-channel analysis filter bank

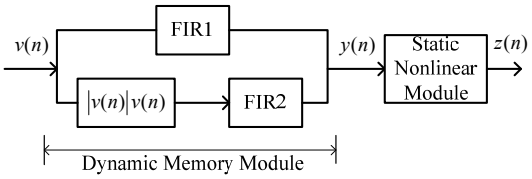

Fig. 6 Block diagram of the augmented Wiener model

Both of the transfer functions of the two FIR filters are as follows:

$$H(z) = 0.3441 + 0.0688z^{-1} + 0.0344z^{-2} + 0.0241z^{-3} + 0.0169z^{-4} + 0.0118z^{-5} \quad (8)$$

The static nonlinear model uses Saleh model [18], whose AM/AM response function $A(r)$ and AM/PM response function $\Phi(r)$ are as follows:

$$A(r) = \frac{\alpha_\alpha r}{1+\beta_\alpha r^2} \qquad \Phi(r) = \frac{\alpha_f r^2}{1+\beta_f r^2} \quad (9)$$

where r is the input signal's amplitude. α_α, β_α, α_f, β_f are model coefficients, and $\alpha_\alpha = 2.1587$, $\beta_\alpha = 1.1517$, $\alpha_f = 4.0033$, $\beta_f = 9.1040$.

Two-carrier WCDMA signal is used as the test signal, the size of LUT is 512, and the tap of each subband FIR filters is 3. The channel number L is 4, and the decimator factor D is 2, which means two times oversampling. The power spectral density (PSD) of PA output in different cases is shown in Fig. 7 for a comparison. In Fig. 7(a), a static Saleh PA and a memoryless LUT predistorter are used, we can see from the figure that the memoryless LUT predistorter can almost completely compensate for the PA's memoryless nonlinear distortion. In Fig. 7(b), the PA model changes to the augmented Wienner model, we can see that the memoryless LUT almost fail to compensate for amplifier's distortion. If keeping LUT unchanging while update subband FIR filters dynamically as the method used in [14], Fig. 7(c) shows that the outcome is almost same as Fig. 7(b). However, if the proposed subband predistorter model and the NG iterative adaptive method are used, Fig. 7(d) shows that the PA's nonlinear distortion is remarkably curbed and the adjacent channel power ratio (ACPR) is reduced by nearly 20dB in the first adjacent channel. In a summary, the comparison results show that the predistortion in [14] is not suitable to compensate for PA's dynamic short-time memory effect, on the contrary, the subband predistortion we proposed in this paper achieves an outstand linearization performance.

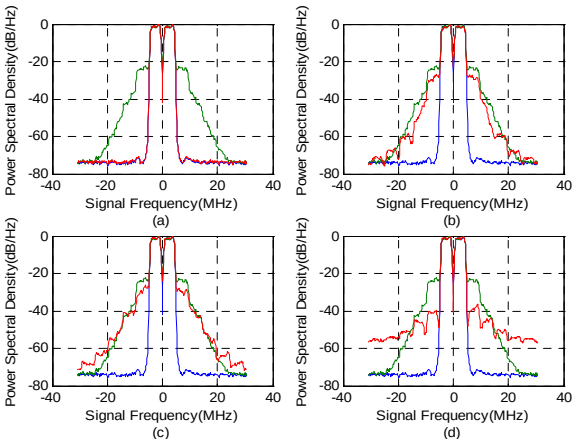

Fig. 7 Power spectral density of PA output（blue line represents signal source， green line represents original PA's Output， red line represents PA's output with predistorter） (a)Memoryless Saleh PA+Memoryless LUT predistorter; (b)Augmented Wienner PA+Memoryless LUT predistorter ; (c) Augmented Wienner PA+Subband predistorter in [14] ; (d) Augmented Wienner PA+Proposed subband predistorter

C. Comparison of the Subband Predistortion and the Full-band Predistortion

The subband predistorter structure can be regarded as an extension of Hammerstein predistorter structure. When the L-channel subband FIR filters merge into a FIR filter, the suband predistorter is equivalent to a conventional Hammerstein full-band predistorter. In this section, we compare the linearization performance and the convergence speed of the subband predistortion and the full-band predistortion. For a fair comparison, the length of the full-band filter is set to be L times of the length of the subband filters.

The simulation uses two-carrier WCDMA signal and the augmented Wienner PA model too. The predistorter coefficients are set as follows: to the subband predistorter, 4-channel CMFB and two times oversampling are used, the size of LUT is 512, and the tap of each FIR is 5; to the full-band predistorter, the size of LUT is 512, and the tap of FIR is 20.

Fig. 8 shows the PSD of the PA output. We can see that the ACPR performance of the subband predistortion outperforms the full-band predistortion, and it indicates that the subband structure can remove memory effects better due to the fact that the decreased bandwidth mitigates the memory effects. In other words, the subband structure can shorten the length of FIR filters effectively.

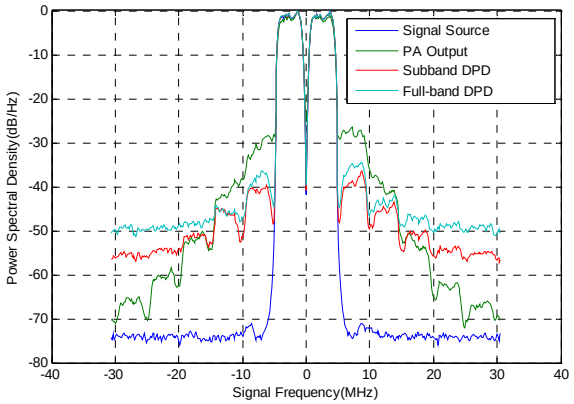

Fig. 8 PSD of the PA with the full-band and the subband predistortion

Another advantage of subband predistortion is that because the subband bandwidth becomes narrower, the subband signals have lower correlation, and the subband adaptive filters have faster convergence speed consequently. The signal correlation can be evaluated by condition number of the input signal's autocorrelation matrix, which is defined as ratio of the maximum eigenvalue of the autocorrelation matrix to the minimum eigenvalue, i.e., $\lambda_{max} / \lambda_{min}$. When the condition number is smaller, the convergence speed of LMS algorithm is faster [19]. Table 1 compares the condition numbers of full-band signals with the subband signals under different filter taps.

Table 1 Condition numbers of full-band and subband signals

Filter Type		Filter Tap	Condition Number ($\lambda_{max} / \lambda_{min}$)
Full-band		12	7.05e+003
4-Channel Subband	Channel 1	3	257.31
	Channel 2	3	8.39
	Channel 3	3	20.91
	Channel 4	3	15.46
Full-band		20	5.86e+006
4-Channel Subband	Channel 1	5	7.59e+004
	Channel 2	5	63.72
	Channel 3	5	305.63
	Channel 4	5	197.94
Full-band		24	8.11e+007
4-Channel Subband	Channel 1	6	8.09e+005
	Channel 2	6	125.53
	Channel 3	6	1.07e+003
	Channel 4	6	660.77

The comparison results of Table 1 show that with the filter tap increasing, the condition number becomes bigger. As a result, under the same iteration step size, the convergence speed of LMS algorithm becomes slower. Furthermore, the condition numbers of the subband decomposed signals are much smaller than the corresponding full-band signal; therefore the convergence property of the subband predistortion is better than the full-band one.

Fig. 9 shows the convergence performance of the full-band predistortion and the subband predistortion. The taps are set to be 5 for the subband filters and 20 for the full-band filter respectively. The iteration step sizes are set to be 0.02. It is obvious that the convergence speed of the subband predistortion is faster than the full-band predistortion. Once convergence, the normalization mean square error (NMSE) of the subband predistortion is about -33.3 dB while the full-band is about -32.6 dB.

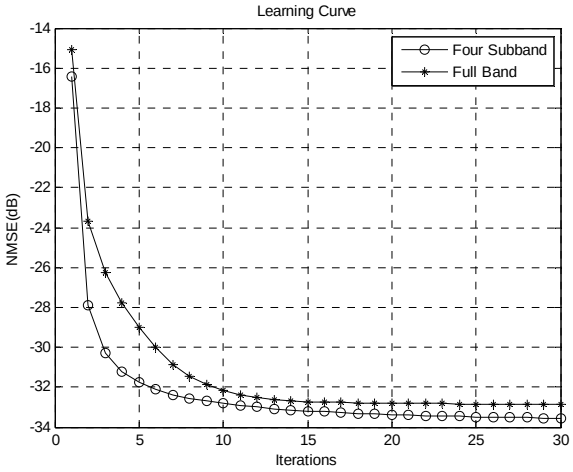

Fig. 9 Convergence curve of the full-band predistortion and the subband predistortion

V. Conclusion

A digital predistorter based on subband decomposition has been introduced in this paper, which consists of an adaptive LUT and an adaptive subband linear filter bank. The Narendra-Gallman iterative algorithm is used to identify the predistorter coefficients of the two modules coordinately. The simulation results show a good linearization performance of the proposed predistorter. Furthermore, compared to a conventional full-band predistortion, the subband architecture accelerates the convergence speed by decreasing signal correlation.

References

[1] J. H. K. Vuolevi, T. Rahkonen and J. P. A. Manninen, "Measurement technique for characterizing memory effects in RF power amplifiers," IEEE Trans. Microw. Theory Tech., vol. 49, no. 8, pp. 1383-1389, 2001.

[2] J. P. Martins, P. M. Cabral, N. B. Garvalho, and J. C. A. Pedro, "Metric for the quantification of memory effects in power amplifiers," IEEE Trans. Microw. Theory Tech., vol. 54, no. 12, pp. 4432-4439, 2006.

[3] P. Roblin, S. K. Myoung, D. Chaillot, Y. G. Kim, A. Fathimulla, J. Strahler and S. Bibyk, " Frequency-selective predistortion linearization of RF power amplifiers," IEEE Trans. Microw. Theory Tech., vol. 56, no. 1, pp. 65-76, 2008.

[4] Y. Ma, Y. Yamao, Y. Akaiwa, "Wideband digital predistortion using spectral extrapolation of band-limited feedback signal," IEEE Trans. Circuits and Systems—I: Regular Papers, vol. 61, no. 7, pp. 2088-2097, 2014.

[5] H. Cao, H. M. Nemati, A. S. Tehrani, T. Eriksson and C. Fager, "Digital predistortion for high efficiency power amplifier architectures using a dual-input modeling approach," IEEE Trans. Microw. Theory Tech., vol. 60, no. 2, pp. 361-369, 2012.

[6] C. D. Presti, D. F. Kimball and P. M. Asbeck, "Close-loop digital predistortion system with fast real-time adaptation applied to a handset WCDMA PA module," IEEE Trans. Microw. Theory Tech., vol. 60, no. 3, pp. 604-618, 2012.
[7] M. Rawat, K. Rawat, F. M. Ghannouchi, "Generalized rational functions for reduced-complexity behavioral modeling and digital predistortion of broadband wireless transmitters," IEEE Trans. Instrum. Meas., vol. 63, no. 2, pp. 485-498, 2014.
[8] D. R. Morgan, Z. Ma, J. Kim, M. G. Zierdt， J. Pastalan, "A generalized memory polynomial model for digital predistortion of RF power amplifiers," IEEE Trans. Signal Process., vol. 54, no. 10, pp. 3852-3860, 2006.
[9] L. Ding, R. Raich and G. T. Zhou, "A Hammerstein predistortion linearization design based on the indirect learning architecture," IEEE International Conference on Acoustics, Speech, and Signal Process., Orlando, USA, pp. III2689-III2692, 2002.
[10] X. Wu and J. Shi, "Adaptive predistortion using cubic spline nonlinearity based Hammerstein modeling," IEICE Trans. Fundamentals, vol. E95. A, no. 2, pp. 542-549, 2012.
[11] J. Moon and B. Kim, "Enhanced Hammerstein behavioral model for broadband wireless transmitters," IEEE Trans. Microw. Theory Tech., vol. 59, no. 4, pp. 924-933, 2011.
[12] P. Jardin and G. Baudoin, "Filter lookup table method for power amplifier linearization," IEEE Trans. Vehicular Tech., vol. 56, no. 3, pp. 1076-1087, 2007.
[13] H. Li, D. H. Kwon, D. Chen and Y. Chiu, "A fast digital predistortion algorithm for radio-frequency power amplifier linearization with loop delay compensation," IEEE Journal of Selected Topics in Signal Process., vol. 3, no. 3, pp. 374-383, 2009.
[14] O. Hammi, S. Boumaiza, M. Jaidance-Saidane and F. M. Ghannouchi, "Digital subband filtering predistorter architecture for wireless transmitters," IEEE Trans. Microw. Theory Tech., vol. 53, no. 5, pp. 1643-1652, 2005.
[15] C. K. Chen and J. H. Lee, "Design of quadrature mirror filters with linear phase in the frequency Domain," IEEE Trans. Circuits and Systems Ⅱ, vol. 39, no. 9, pp. 593-605, 1992.
[16] D. Zenobio, G. Santella and F. Mazzenga, "Adaptive linearization of power amplifier in orthogonal multicarrier schemes," IEEE Int. Wireless Communication System Symposium, NY USA, pp. 225- 230, Nov. 1995.
[17] T. Liu, S. Boumaiza and F. M. Ghannouchi, "Augmented Hammerstein predistorter for linearization of broad-band wireless transmitters," IEEE Trans. Microw. Theory Tech., vol. 54, no. 4, pp. 1340-1349, 2006.
[18] A. Saleh, "Frequency-independent and frequency-dependent nonlinear model models of TWT amplifiers," IEEE Trans. Commun., vol. 29, no. 11, pp. 1715-1720, 1981.
[19] S. Harkin, "Adaptive filter Theory, 3rd ed.," Prentice-Hall: Englewood Cliffs, N. J., 1996.

Xiaofang Wu received the B.S. and the M.S. degrees in electronic engineering from Xiamen University, China, in 1993 and 1997 respectively, and the Ph. D. degree in communication and information systems from Xiamen University in 2011. She is currently an associate professor with the School of Information Science and Technology, Xiamen University, China. Her research interests are in the predistortion linearization of nonlinear power amplifiers for wireless applications, analog circuits design, and wireless communication signal processing.

Miao Xiong received the B.S. degree in electronic information engineering from Nanjing Agricultural University, 2013. He is a master degree candidate at Xiamen University, China. His research interest is digital predistortion for power amplifiers.